

タイトル	著者	グループ	雑誌	巻	番号	頁	年
Voriconazoleの概要	河野 茂	呼吸器感染症	日本化学療法学会雑誌	53		1-3	2005

【総説】

Voriconazole の概要

河野 茂

長崎大学大学院感染分子病態学講座 (第二内科)*

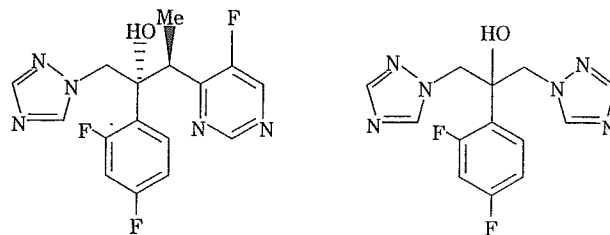
(平成 17 年 7 月 8 日受付・平成 17 年 8 月 22 日受理)

Voriconazole (VRCZ) は、日本では 2005 年 4 月に承認された新しいトリアゾール系抗真菌薬である。バイオアベイラビリティの高さと広範な抗真菌スペクトルが特徴であり、従来の抗真菌薬が効きにくい *Candida glabrata*, *Candida krusei*, ならびにアスペルギルス属, フサリウム属, スケドスポリウム属にも抗真菌作用を発揮する。注射薬と経口薬の両剤形があるため、静注療法から経口療法への切り替えも可能である。深在性真菌症の感染部位となる肺, 肝, 腎, 脳, 眼などへの組織移行性に優れている。VRCZ の血清中濃度は個人差が大きい, 血清中濃度と有効性・安全性との相関は見出されていない。造血幹細胞移植 (HSCT) 例での深在性真菌症の治療には、日本では現在フルコナゾールまたはアムホテリシン B が用いられているが、VRCZ は、特にアスペルギルス症の治療での有効性が期待されている。深在性真菌症に VRCZ を使用した日本の第 III 相臨床試験では、VRCZ は忍容性が良好であり、アスペルギルス症, カンジダ症, クリプトコックス症において優れた有効性が確認され、侵襲性肺アスペルギルス症にも有効であった。HSCT 後の免疫抑制患者に発症した侵襲性アスペルギルス症に VRCZ とアムホテリシン B を使用した海外の試験では、VRCZ のほうが有意に高い有効性を示した。VRCZ は、わが国の深在性真菌症治療を一新する可能性をもち、今後の深在性真菌症の治療において優れた臨床効果を示すことが期待されている。

Key word: voriconazole (VRCZ)

近年、深在性真菌症の発症頻度は全世界的に増加している¹⁾。この背景には、ステロイド薬や抗悪性腫瘍薬での治療による免疫抑制患者の増加や、侵襲的な医療機器の使用の普及などの医療技術の革新がある。また、深在性真菌症の原因真菌の種類にも、変化が認められている。日本病理剖検輯報における内臓真菌症の発症頻度では²⁾、1970~1980 年代はカンジダ症が最も高頻度であったが、1989 年にトリアゾール系抗真菌薬 fluconazole (FLCZ) が発売されたこともあり、1990 年以降にはアスペルギルス症が第一位を占めるようになっている。アスペルギルス症のなかでも、侵襲性アスペルギルス症は難治症例が多く、早期診断法および有効性の高い治療法の研究が必要とされる。現在、わが国で使用可能な抗真菌薬は、ポリエンマクロライド系薬では amphotericin B (AMPH-B)、ピリミジン誘導体では flucytosine (5-FC)、イミダゾール系薬では micafungin (MCFG) の 7 薬剤である。これらのなかでアスペルギルス属に対して抗真菌活性を示すのは、AMPH-B, ITCZ および MCFG の 3 薬剤であるが、副作用プロフィール、抗真菌活性などが改善され、さらに臨床におけるエビデンスをも有する新規抗真菌薬の登場が求められていた。

Voriconazole (VRCZ) は、英国ファイザー中央研究所で創



Voriconazole

Fluconazole

Fig. 1. Chemical structure of voriconazole.

薬された新規トリアゾール系抗真菌薬であり、欧州では 2002 年 3 月に、米国では 2002 年 5 月に承認されている。本薬剤は FLCZ の誘導体であり (Fig. 1)、FLCZ の有用な特徴を有しながら、FLCZ よりも強力で広範囲スペクトルの抗真菌作用を示すのが特徴である。すなわち、FLCZ 低感受性の *Candida glabrata* および *Candida krusei* に対しても優れた抗真菌活性を示すと同時に、アスペルギルス属, フサリウム属, スケドスポリウム属に対しては殺真菌作用を示す。さらに FLCZ と同様に、組織移行性が高く、注射薬と経口薬の両剤形があるためスイッチ療法も可能である。わが国では、1996 年から第 I 相試験、2000 年より第 III 相試験が実施され、2005 年 4 月には

*長崎県長崎市坂本町 1-7-1

承認が得られている。

本誌では、第51回日本化学療法学会東日本支部総会(2004年10月、新潟)にて開催されたVRCZ新薬シンポジウムに基づき、血液内科領域における深在性真菌症の実態とVRCZ発売後の位置づけを概説し、本薬剤の開発の経緯、抗真菌活性、薬物動態およびわが国・欧米での臨床試験などの試験結果についてまとめた。

I. 深在性真菌症の実態

わが国での血液内科領域における深在性真菌症の実態は、臨床試験およびアンケート調査によって明らかにされている¹⁾。急性骨髄性白血病患者に対する臨床試験および造血幹細胞移植についてのアンケート調査によると、アスペルギルス属、カンジダ属を中心とした真菌感染がみられ、その死亡率の高さが問題となっていた²⁾。白血病患者に対する抗真菌薬療法についてのアンケート調査の結果、予防的投与ではFLCZ(41%)およびAMPH-B(42%)が多く選択され、経験的治療ではFLCZが66%に用いられていた³⁾。また、アスペルギルス症の標的治療ではAMPH-Bが主に用いられていたが、十分量を投与されているとはいえない状況であった(0.5 mg/kg: 84%, 0.7 mg/kg: 21%, ≥ 1 mg/kg: 40%)。抗真菌療法におけるVRCZの位置づけは、特に経験的治療や、カンジダ属、アスペルギルス属に対する標的治療薬として期待されている。

II. 作用機序および真菌学的効果

VRCZの作用機序は、既存のトリアゾール系薬と同様で、真菌細胞の主要な細胞膜成分であるエルゴステロール生合成に必須のCYP450依存lanosterol-14 α -demethylaseを阻害することにより抗真菌活性を示す。本薬剤のエルゴステロール生合成阻害作用は*Candida albicans*や*Aspergillus fumigatus*などの病原真菌に選択的で、そのIC₅₀比はITCZの約3倍であった。VRCZのMIC₉₀はカンジダ属に対して0.063~0.5 μ g/mL、*A. fumigatus*に対して0.5 μ g/mLと優れた抗真菌活性を示した。さらに、VRCZはアスペルギルス属に対してMICの2倍の濃度で殺真菌効果を示した。モルモットのアスペルギルス属全身感染モデルおよび肺感染モデルに対しては、臓器治癒率および生菌数減少効果ともにITCZより優れていた。

III. 薬物動態

VRCZには注射薬と経口薬の両剤形があり、bioavailabilityは約96%と高いなど、薬物動態学的特徴をいくつか有している。経口薬の吸収は、ITCZと異なり、胃内pHの変化に影響されない。経口投与、静脈内投与ともに初日のみ負荷投与(ローディングドーズでの投与)を行うことで、4日目に定常状態となる。半減期は約6時間である。また、組織移行性にも優れ、その濃度は主要真菌のMICを上回っており、深在性真菌症が好発する肺、肝、脾、腸、腎などの組織に対して、血漿中濃度を上回る優

れた組織移行性が確認された。

VRCZは、CYP2C9、CYP2C19、CYP3A4によって代謝されるが、CYP2C19には遺伝子多型が存在し、薬物代謝の個人差の一因と考えられている。日本人では低い代謝酵素活性を有する人(PM: Poor Metabolizer)が19%を占め、第I相試験において遺伝子系別に血漿中VRCZ濃度を検討した結果、PMでは血漿中VRCZ濃度が高いことがわかった。ただし、同じ遺伝子系のなかでも、個人差が大きいことから、遺伝子系による用量調節はあまり意味がないと考えられる。小児患者においては、成人と比べて血漿中VRCZ濃度が低いが、これは、小児では酵素活性が高くクリアランスが速いためと考えられる。

IV. 臨床効果

本薬剤の国内第III相臨床試験では、深在性真菌症患者100例にVRCZを投与し、臨床的有用性(有効性および安全性)を検討した。VRCZの投与は、静注療法では負荷投与として投与1日目に6 mg/kgを2回、2日目から5~7日目までは重篤な真菌症の場合は4 mg/kgを1日2回投与、それ以外は3 mg/kgを1日2回投与した。経口療法では負荷投与として1日目に300 mgを2回、2日目から5~7日目までは150~200 mgを1日2回投与した。また、静注療法を3日間行った後、静注療法から経口療法への切り替え(スイッチ療法)を可能とした。その結果、アスペルギルス症、カンジダ症、クリプトコックス症において優れた有効性が確認され、予後が悪いとされる侵襲性肺アスペルギルス症に対しても満足すべき結果が得られた。また十分な忍容性が認められた。特徴的な副作用として視覚障害がみられた。VRCZの血漿中濃度は個人差が大きいが、血漿中VRCZ濃度と有効性・安全性との相関はみられなかった。

また、海外においては、造血幹細胞移植例および急性白血病などの免疫不全状態にある患者に発症した侵襲性アスペルギルス症を対象として実施されたVRCZとAMPH-Bの無作為化比較試験が報告されている⁴⁾。12週後の有効率はVRCZ群52.8%、AMPH-B群31.6%であり、VRCZ群のほうが有意に優れており、12週後の生存率でもVRCZ群71.2%、AMPH群58.2%と、VRCZ群のほうが有意に高値であった。

VRCZは、わが国の深在性真菌症治療を一新する可能性のある新規抗真菌薬であり、今後の深在性真菌症の治療において優れた臨床効果を示すことが期待されている。

文 献

- 1) Marr K A, Carter R A, Crippa F, et al: Epidemiology and outcome of mould infections in hematopoietic stem cell transplant recipients. Clin Infect Dis 34: 909, 2002
- 2) 久米 光, 阿部美知子: 肺真菌症の疫学。臨床と微生物 27: 133~139, 2000
- 3) 正岡 徹: 白血病治療に合併する真菌感染症の Em-

piric Therapy—日本におけるコンセンサスを求めて—。Jap J Antibio 50: 669~682, 1997

4) Herbrecht R, Denning D W, Patterson T F, et al: Vori-

conazole versus amphotericin B for primary therapy of invasive aspergillosis. N Engl J Med 347: 408, 2002

Overview of Voriconazole

Shigeru Kohno

Division of Molecular & Clinical Microbiology, Department of Molecular Microbiology & Immunology, Nagasaki University Graduate School of Medicine, 1-7-1 Sakamoto, Nagasaki, Japan

Voriconazole (VRCZ) is a new triazole antifungal agent that was approved in Japan in April 2005. VRCZ is characterized by a high bioavailability and a broad spectrum of antifungal activity that includes a number of species that are refractory to other currently available antifungals, such as *Candida glabrata* and *Candida krusei* as well as *Aspergillus*, *Fusarium*, and *Scedosporium* species. VRCZ is available in both intravenous and oral formulations, facilitating a smooth switch from drip infusion to oral therapy. It shows excellent penetration into tissues that are sites of deep-seated mycoses, such as the lung, liver, kidney, brain and eyes. Although serum VRCZ concentrations may vary greatly, no correlation has been found between serum concentrations and efficacy or safety. For the treatment of deep-seated mycoses in patients with hematopoietic stem cell transplantation (HSCT), which is currently treated in Japan using fluconazole or amphotericin B, VRCZ is anticipated to be particularly effective for empiric and targeted therapy. A phase III clinical trial in Japan of VRCZ for the treatment of deep-seated mycoses showed that VRCZ was well tolerated and was extremely effective against aspergilloses, candidiasis, and cryptococcosis as well as against invasive pulmonary aspergillosis. An international trial of VRCZ and amphotericin B for the treatment of invasive aspergilloses that developed in immunocompromised patients after HSCT showed that VRCZ was significantly more effective. VRCZ promises to improve the treatment of deep-seated mycoses in Japan and is expected to exhibit excellent clinical effects in the future treatment of this condition.

Fluconazole Treatment Is Effective against a *Candida albicans* *erg3/erg3* Mutant In Vivo Despite In Vitro Resistance

Taiga Miyazaki,^{1,2} Yoshitsugu Miyazaki,^{1*} Koichi Izumikawa,¹ Hiroshi Kakeya,¹
Shunichi Miyakoshi,³ John E. Bennett,² and Shigeru Kohno¹

Second Department of Internal Medicine, Nagasaki University School of Medicine, 1-7-1 Sakamoto, Nagasaki 852-8501,¹
and Lead Discovery Research Laboratories, Sankyo Co., Ltd., Tokyo,³ Japan, and Clinical Mycology Section,
Laboratory of Clinical Infectious Diseases, National Institute of Allergy and Infectious Diseases,
National Institutes of Health, Bethesda, Maryland²

Received 13 October 2005/Returned for modification 7 November 2005/Accepted 23 November 2005

Candida albicans *ERG3* encodes a sterol C5,6-desaturase which is essential for synthesis of ergosterol. Defective sterol C5,6 desaturation has been considered to be one of the azole resistance mechanisms in this species. However, the clinical relevance of this resistance mechanism is still unclear. In this study, we created a *C. albicans* *erg3/erg3* mutant by the “Ura-blaster” method and confirmed the expected azole resistance using standard in vitro testing and the presence of ergosta-7,22-dien-3 β -ol instead of ergosterol. For in vivo studies, a wild-type *URA3* was placed back into its native locus in the *erg3* homozygote to avoid positional effects on *URA3* expression. Defective hyphal formation of the *erg3* homozygote was observed not only in vitro but in kidney tissues. A marked attenuation of virulence was shown by the longer survival and the lower kidney burdens of mice inoculated with the reconstituted Ura⁺ *erg3* homozygote relative to the control. To assess fluconazole efficacy in a murine model of disseminated candidiasis, inoculum sizes of the control and the *erg3* homozygote were chosen which provided a similar organ burden. Under these conditions, fluconazole was highly effective in reducing the organ burden in both groups. This study demonstrates that an *ERG3* mutation causing inactivation of sterol C5,6-desaturase cannot confer fluconazole resistance in vivo by itself regardless of resistance measured by standard in vitro testing. The finding questions the clinical significance of this resistance mechanism.

Candida albicans is the most common cause of deep mycoses in humans. Azole therapy has been well tolerated and effective for many forms of candidiasis. Of concern is that long-term azole treatment of oropharyngeal candidiasis in human immunodeficiency virus-infected patients has encountered progressive azole resistance (14, 40). Azole antifungals inhibit the biosynthesis of ergosterol, the major sterol of cell membrane, by targeting lanosterol 14 α -demethylase encoded by *ERG11* (38). Alteration of amino acid composition of lanosterol 14 α -demethylase (37), increased drug efflux (32, 34), and altered ergosterol synthetic pathways due to blockage of sterol C5,6-desaturase encoded by *ERG3* (17, 33) have been known as factors contributing to azole resistance in *C. albicans* and *Saccharomyces cerevisiae* (for reviews, see references 1 and 35). However, no relation between defective sterol C5,6-desaturase and azole resistance was found in *Candida glabrata* (9). The relevance of azole resistance in *C. albicans* *erg3* mutants is still unclear. Although it has been reported that a few azole-resistant clinical isolates of *C. albicans* exhibited a sterol profile indicative of defective sterol C5,6 desaturation (4, 18, 26), the possibility remains that another mechanism(s) of azole resistance might have been present in those isolates. For instance, the Darlington strain, an *erg3/erg3* mutant isolated from the oral cavity, was also azole resistant due to mutations in *ERG11* (15, 24).

A mechanism by which *erg3* mutations cause azole resistance has been proposed but is in part counterintuitive. The sterol composition of these mutants is largely ergosta-7,22-dien-3 β -ol rather than ergosterol. The only difference between these molecules is the saturation of the C5-6 bond in ergosta-7,22-dien-3 β -ol. Substitution of ergosta-7,22-dien-3 β -ol for ergosterol in the cell membrane leads to increased, not decreased, sensitivity to a large number of toxic chemicals, detergent, ions, and low pH (11, 33). The contrary effect of increased azole resistance has been hypothesized to be due to the ability of the cell to circumvent the azole inhibition of C14 demethylation by successfully utilizing C14-methylated C5,6-saturated sterols (17, 18). What is not clear from these studies is whether this azole resistance in vitro translates into a decreased therapeutic response to azoles in vivo, particularly considering the increased fragility of the *erg3* mutants.

Very recently, it has been reported that two clinical *C. albicans* isolates exhibiting defective activity of sterol C5,6-desaturase in their sterol compositions showed reduced virulence in mice and impaired hyphal formation in vitro compared to azole-susceptible clinical isolates (4). In addition, attenuated virulence of a laboratory strain (*erg3 Δ ::hisG/erg3 Δ ::hisG-URA3-hisG erg11 Δ ::hisG/ERG11*) generated by the “Ura-blaster” technique was shown (4). Although “Ura-blaster” is a useful method for gene disruption in *C. albicans*, a positional change of *URA3* affects the expression level and activity of Ura3p, orotidine 5'-monophosphate decarboxylase (3, 19, 36). Because reduced *URA3* expression itself attenuates virulence of *C. albicans* (3, 19, 36), effects of a gene disruption on virulence should be evaluated under the same conditions for the *URA3*

* Corresponding author. Mailing address: Second Department of Internal Medicine, Nagasaki University School of Medicine, 1-7-1 Sakamoto, Nagasaki 852-8501, Japan. Phone: 81-95-849-7273. Fax: 81-95-849-7285. E-mail: ym46@net.nagasaki-u.ac.jp.

TABLE 1. *C. albicans* strains used in this study

Strain	Genotype	Reference
CAF2-1	<i>iro1-ura3Δ::imm434/IRO1 URA3</i>	8
CAI-4	<i>iro1-ura3Δ::imm434/iro1-ura3Δ::imm434</i>	8
CAD1U	<i>erg3Δ::hisG-URA3-hisG/ERG3 iro1-ura3Δ::imm434/iro1-ura3Δ::imm434</i>	This study
CAD1	<i>erg3Δ::hisG/ERG3 iro1-ura3Δ::imm434/iro1-ura3Δ::imm434</i>	This study
CAE3DU	<i>erg3Δ::hisG-URA3-hisG/erg3Δ::hisG iro1-ura3Δ::imm434/iro1-ura3Δ::imm434</i>	This study
CAE3D	<i>erg3Δ::hisG/erg3Δ::hisG iro1-ura3Δ::imm434/iro1-ura3Δ::imm434</i>	This study
CAE3DU3	<i>erg3Δ::hisG/erg3Δ::hisG iro1-ura3Δ::imm434/IRO1 URA3</i>	This study

locus. To avoid positional effects on *URA3* expression, reintroduction of *URA3* into its original locus or an appropriate expression locus such as the *RPS10* locus has been suggested (3, 36). For our in vivo studies, therefore, a wild-type *URA3* was placed back into its native locus in the *erg3* homozygote, and this allowed us to use a well-known control strain, CAF2-1 (8), which is derived from the wild-type isolate SC5314 (10) and is also a *ura3/URA3* heterozygote. Here, we present a detailed evaluation of the *erg3* mutant phenotype in *C. albicans* and cast doubt on the clinical relevance of this mechanism of resistance.

MATERIALS AND METHODS

Strains and culture conditions. The *C. albicans* strains used in this study are listed in Table 1. The *C. albicans* strains were routinely propagated in yeast peptone dextrose (YPD) medium (1% yeast extract, 2% peptone, 2% dextrose). The *URA3* transformants were selected on minimal (MIN) (0.7% yeast nitrogen base without amino acid, 2% glucose) agar plates. The *ura3* auxotrophs were obtained on MIN agar plates containing 0.1% 5-fluoroorotic acid (5-FOA; Lancaster, Pelham, NH) and 50 μg/ml uridine (8). Agar (1.5%) was added for solid media. RPMI 1640 medium was buffered with 0.165 M morpholinopropanesulfonic acid and was adjusted to pH 7.0. When needed, 50 μg/ml uridine was added. *Escherichia coli* strains were grown in Luria-Bertani medium containing 100 μg/ml ampicillin at 37°C.

Strain construction. All PCR products used in plasmid construction were sequenced before use. Transformation in *C. albicans* was performed by electroporation (Gene Pulser; Bio-Rad Laboratories, Richmond, CA) as described previously (39).

(i) **Disruption of *ERG3*.** The 5' end (0.3 kb) of the *ERG3* open reading frame (ORF) was amplified with primers Tg1 (5'-ATGGATATCGTACTAGAAATT TGTG-3') and Tg4 (5'-GCTGGGAAAATTTAGGAGC-3') from genomic DNA of strain CAI-4 (8). The PCR product was inserted into the BglII site of a plasmid containing the *hisG-URA3-hisG* cassette, p5921 (8), to yield pE3DC1. The 3' end (0.4 kb) of the *ERG3* ORF was obtained with primers Tg2 (5'-TC ATTGTCAACATATTCTCTATCG-3') and Tg3 (5'-TCCAGTTGATGGGT TCTTCC-3') and inserted into the BamHI site of pE3DC1 to yield pE3DC2. Amplified DNA products and digested fragments of p5921 and pE3DC1 were blunt ended (DNA Blunting kit; Takara) before ligation. The orientation of the inserted PCR products of *ERG3* ORF 5' and 3' regions was verified at each step by PCR with primer pairs Tg1 and K11 (*URA3* specific) (5'-GCTAACATCAA TAACCTCTTGGC-3') for pE3DC1 and K10 (*URA3* specific) (5'-CTGAGC AACAACCCATACACAC-3') and Tg2 for pE3DC2, respectively. Ten million CAI-4 cells were transformed with 2 μg of a 5-kb SacI-PstI fragment excised from pE3DC2. *Ura*⁺ transformants were obtained on MIN agar plates, and then *Ura*⁻ isolates resulting from *cis* recombination between the *hisG* repeats were selected using 5-FOA (8). We performed sequential disruption of the *C. albicans* *ERG3* gene by using the *Ura*-blaster technique again to yield *erg3/erg3* strains.

(ii) **Reintegration of *URA3*.** A 5-kb BglII-PstI fragment containing the *IRO1-URA3* locus (5, 20) was obtained from pLUBP, a kind gift from William A. Fonzi. Plasmid pLUBP consists of a pLITMUS28 backbone with a 5-kb BglII-PstI insert obtained from pUR3 (16). The *Ura*⁻ *erg3/erg3* strain, CAE3D, was transformed with 1 μg of this 5-kb fragment to place wild-type *URA3* back into its original locus as described previously (5, 20). Transformants were selected by *Ura* prototrophy. Homologous recombination and no ectopic integration of the transforming DNA were confirmed by Southern blotting.

Growth rates. The growth rates of *C. albicans* strains were examined by the optical density at 600 nm (OD₆₀₀) every hour. Tested media included YPD,

MIN, yeast peptone glycerol (1% yeast extract, 2% peptone, 3% glycerol, 1% ethanol), and RPMI 1640, and tested growth temperatures included 25, 30, 37, 40, and 42°C. An overnight culture grown at 30°C was diluted 1 to 500 into each medium, and then the cultures were incubated in 250-ml flasks with shaking at 200 rpm.

Antifungal susceptibility assay. Logarithmic-phase cultures were obtained by preculture in YPD medium. Cells were harvested, washed, and adjusted to the desired concentrations by counting the number of cells with a hemocytometer. Antifungal susceptibility assay was performed according to the M27-A2 standard protocol approved by the National Committee of Clinical Laboratory Standards (NCCLS) (25). Tested antifungal agents were fluconazole (Pfizer, Inc.), itraconazole (Janssen Pharmaceuticals), miconazole (Mochida, Inc.), and voriconazole (Pfizer, Inc.). RPMI 1640 medium adjusted to pH 7.0 was used. Cells were incubated in 96-well U-bottom microtiter plates at 35°C, and the OD₆₀₀ was measured by a microplate spectrophotometer (Benchmark Plus; Bio-Rad Laboratories) at 24 and 48 h. The MIC₅₀ was defined as the drug concentration required for 50% growth inhibition compared to that in the drug-free culture. Fluconazole susceptibility was also evaluated by Etest (AB Biodisk, Solna, Sweden) according to the manufacturer's instructions.

Sterol analysis. Sterol identification was made by gas chromatography-mass spectrometry (Hewlett Packard 6890/5973) using a DB5 capillary column (15 m by 0.25 mm; J&W Scientific), essentially as described previously (2, 13).

Southern and Northern blot analysis. Southern blot analysis was performed following the standard protocol (30). The genomic DNA was digested with SalI and PstI. The 0.4-kb PCR product of the 3' end of the *ERG3* ORF (described above) was used as an *ERG3* probe to monitor the recombination events. Both pre- and post-5-FOA isolates were also verified using an *URA3* probe, which was obtained by PCR with primers K10 and K11 from p5921. The genomic DNA of the reconstituted *Ura*⁺ *erg3/erg3* strain, CAE3DU3, was digested with HindIII and hybridized with the *URA3* probe.

Northern blot analysis was performed following the methods described previously (41). Briefly, logarithmic-phase cultures at an OD₆₀₀ of 0.75 were reincubated at 35°C in the absence and the presence of fluconazole at a concentration of 0.25 μg/ml. Total RNA was extracted when the culture reached an OD₆₀₀ of 1.0 (approximately 90 min of incubation). An *ERG3* probe for Northern blotting was amplified with primers designed in the deleted region of *ERG3* ORF, Tg10 (5'-GGAAGAACCCATCAACTGGATGG-3') and Tg11 (5'-GTGCCACTAC TGCCATTCCA-3'). Gene probes for *ERG11*, *CDR1*, and *MDR1* were amplified with primers described previously (12). Autoradiography was analyzed with a Fujix BAS-5000 image analyzer (Fuji Photo Film, Tokyo, Japan).

In vitro morphology assay. To induce hyphal growth, stationary-phase cells grown in YPD medium at 30°C were plated at approximately 100 cells/plate on spider agar (21), on 10% human serum agar, and on RPMI 1640 medium with 10% human serum agar. YPD agar was used as a control. Plates were incubated at 37°C. The cells were also grown in liquid RPMI 1640 medium in the absence and the presence of 10% human serum under the same conditions as those of the MIC assay. All tested media were adjusted to pH 7.0. Cell morphology was examined after 18-, 48-, and 72-h incubations.

In vivo studies. Female, 8-week-old, BALB/c mice (Charles River Laboratories, Danvers, MA) were used in all experiments. Mice were maintained according to National Institutes of Health guidelines for animal care and in fulfillment of American Association for Accreditation of Laboratory Animal Care criteria (6). *C. albicans* strains for inoculation were grown in YPD medium at 30°C. Logarithmic-phase cells were harvested, washed, resuspended in sterile saline, and adjusted to the desired concentrations by counting the number of cells with a hemocytometer. Actual CFU in the inocula were determined by culturing serial dilutions of each preparation onto YPD plates. Mice were inoculated with a volume of 0.2 ml via the lateral tail vein.

TABLE 2. Antifungal susceptibilities of *C. albicans* strains

Strain (genotype)	MIC ₅₀ (μg/ml) ^a of:			
	Fluconazole	Itraconazole	Miconazole	Voriconazole
CAF2-1 (<i>ERG3/ERG3 ura3/URA3</i>)	0.125	0.125	0.5	0.016
CAI-4 (<i>ERG3/ERG3 ura3/ura3</i>)	0.25	0.125	0.5	0.016
CAD1 (<i>erg3/ERG3 ura3/ura3</i>)	0.25	0.5	0.5	0.03
CAE3D (<i>erg3/erg3 ura3/ura3</i>)	>64	>16	>16	>16
CAE3DU3 (<i>erg3/erg3 ura3/URA3</i>)	>64	>16	>16	>16

^a Antifungal susceptibility was examined by broth microdilution tests following the NCCLS M27-A2 protocol (25), and MIC was determined as the drug concentration required for 50% growth inhibition compared to the drug-free culture at 48 h.

(i) **Monitoring of survival.** Forty mice were divided into four groups. Ten mice of each group were injected with a higher or a lower inoculum of either CAF2-1 (*ERG3/ERG3 ura3/URA3*) or CAE3DU3 (*erg3/erg3 ura3/URA3*) on day 0 of the experiment. The mice were observed twice daily until day 24.

(ii) **Kidney CFU assay.** Twenty mice per group were injected with either CAF2-1 or CAE3DU3 on day 0 of the experiment. In each group, kidneys were removed from three mice euthanized on days 2 and 7 and from four mice on day 4. To assess fungal burden in tissue, the excised kidneys were weighed individually and homogenized in sterile saline by using a Precision Tissue Grinder (Kendall, Mansfield, MA). Aliquots of 100 μl from kidney homogenates and their dilutions of 10⁻¹ and 10⁻² were plated onto YPD agar. Colonies were counted after 3 days of incubation at 30°C, and CFU per gram of kidney were calculated. The remaining 10 mice in each group were monitored for survival until day 24 of the experiment.

(iii) **Histopathologic analysis.** Three mice per group were injected with CAF2-1 or CAE3DU3 on day 0 of the experiment. Both kidneys were excised on day 4 and fixed in 10% neutral buffered formalin. Paraffin-embedded tissue sections were stained with Grocott-Gomori methenamine silver stain. Tissues were microscopically examined for morphology of *C. albicans* cells.

(iv) **Fluconazole treatment.** Twenty mice per group were injected with either CAF2-1 or CAE3DU3 on day 0 of the experiment. The mice were treated with fluconazole (Diflucan; Pfizer, Inc.) given by gavage at 40 mg/kg of body weight once a day for 4 days, starting at 3 h after inoculation. As a control, mice were treated with the equivalent volume (0.2 ml/gavage) of sterile saline. Kidneys were excised from all mice on day 4 of the experiment, and kidney CFU were determined as described above.

Statistical analysis. Multivariate regression analyses with log CFU as the dependent variable were used to assess the difference between the two groups in the in vivo virulence assay. The estimated group difference in log CFU and its associated 95% confidence intervals are presented. F tests were used to derive *P* values for assessing the significance of the group. Log-rank tests were used to compare the survival rates of mice. In the [³H]fluconazole accumulation assay and the in vivo fluconazole treatment experiment, Student's *t* test was used to analyze differences between mean values of groups of data. A significance level of 0.05 was used to determine statistical significance. All analyses were conducted using STATA version 8.2 (STATA Corp., College Station, TX).

RESULTS

Creation of *erg3* disruptants and an *ERG3* reintegrant. Both copies of *ERG3* in *C. albicans* strain CAI-4 (8) were disrupted sequentially by means of the Ura-blaster technique and 5-FOA selection, yielding the following strains: the Ura⁺ *erg3/ERG3* strain (CAD1U), Ura⁻ *erg3/ERG3* strain (CAD1), Ura⁺ *erg3/erg3* strain (CAE3DU), and Ura⁻ *erg3/erg3* strain (CAE3D) (Table 1). Each strain construction was confirmed by Southern blotting with the *ERG3* or the *URA3* probe (data not shown). The *IRO1-URA3* locus of CAE3D was reconstituted by transformation with a 5-kb BglII-PstI fragment of pLUBP. Southern blotting with the *URA3* probe confirmed that a copy of *URA3* was placed back to its native locus in the reconstituted Ura⁺ *erg3/erg3* strain, CAE3DU3 (data not shown).

Susceptibility phenotypes of the *erg3* disruptants. We examined the effect of *ERG3* disruption on the growth rate of *C.*

albicans before performing susceptibility assays. As representative data, doubling times of each strain in YPD medium at 30°C were as follows: 100 min for CAF2-1 and CAE3DU3, 123 min for CAD1U and CAE3DU, and 145 min for CAI-4, CAD1, and CAE3D. The increases in doubling times were due to an ectopic expression of *URA3* at the *ERG3* locus (CAD1U and CAE3DU) and uracil auxotrophy (CAI-4, CAD1, and CAE3D). The growth ability of *C. albicans* was not affected by *ERG3* disruption under the various conditions, including different media and growth temperatures (25, 37, 40, and 42°C) as described in Materials and Methods.

Antifungal susceptibilities of the *erg3* disruptants were determined by broth dilution tests following the NCCLS M27-A2 protocol (25) (Table 2). Although heterozygous disruption of *ERG3* did not affect antifungal susceptibilities, the *erg3* homozygotes CAE3D and CAE3DU3 were found to be resistant to fluconazole in RPMI 1640 medium with a MIC of >64 μg/ml and were also resistant to other azoles, such as itraconazole (MIC, >16 μg/ml), miconazole (MIC, >16 μg/ml), and voriconazole (MIC, >16 μg/ml). The absence of *URA3* did not affect the antifungal susceptibilities.

Some fluconazole-resistant *C. albicans* isolates have been shown to exhibit significant trailing growth, which is also known as a low-high MIC phenotype (23, 29). Fluconazole MICs for strains having this type of growth appear to be low at 24 h but are much higher at 48 h. To examine whether the low-high MIC phenotype can be seen in the *erg3* homozygote, the fluconazole MIC was measured at 24 and 48 h (Fig. 1). Although the optical density of the growth control was relatively low at 24 h, the *erg3* homozygote, CAE3DU3, consistently showed fluconazole resistance with a MIC of >64 μg/ml at both 24 and 48 h. The fluconazole MIC of CAE3DU3 was also measured by Etest and was >256 μg/ml at both 24 and 48 h; meanwhile, that of the control strain, CAF2-1, was 0.25 μg/ml at 24 h and 0.38 μg/ml at 48 h.

Effects of the *ERG3* disruption on sterol contents in the cell membrane. We confirmed the phenotypes of the *erg3* hetero- and homozygotes by sterol assay (Table 3). Sterol contents of the *erg3* heterozygote, CAD1, were similar to those of CAI-4. On the other hand, in the *erg3* homozygote CAE3D, ergosta-7,22-dien-3β-ol accumulated in place of ergosterol and no C5,6-desaturated sterols were detected. The presence of *URA3* did not affect sterol composition (data not shown). The sterol profile of CAE3D was consistent with that of the previously reported *C. albicans erg3* mutant (*erg11/ERG11 erg3/erg3*) (33).

Northern blot analysis of *ERG3*, *ERG11*, and drug efflux pump genes. Northern blot analysis of CAE3DU confirmed

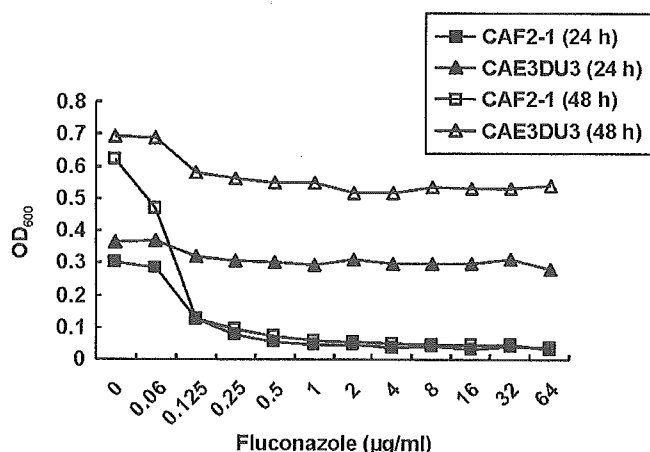


FIG. 1. Fluconazole susceptibility of a *C. albicans* *erg3* homozygote at 24 and 48 h. Fluconazole susceptibility of CAF2-1 (*ERG3/ERG3 ura3/URA3*) and CAE3DU3 (*erg3/erg3 ura3/URA3*) was examined by broth microdilution tests following the NCCLS M27-A2 protocol (25). The optical density at 600 nm (OD₆₀₀) was measured at 24 and 48 h of incubation. The assay was performed in triplicate, and representative data are shown.

the lack of *ERG3* transcript and the increased *ERG11* expression compared to that of CAF2-1 and CAD1U (Fig. 2). We sequenced *ERG11* in the *erg3* homozygote, CAE3D, and found no difference from published sequence data. In addition, there was no difference in expression levels of *CDR1*, an ATP-binding cassette transporter gene (34), in the presence of fluconazole among CAF2-1, CAD1U, and CAE3DU (data not shown). *MDR1*, a gene encoding a membrane transport protein of the major facilitator superfamily (34), was not expressed detectably in any of the strains (data not shown).

Morphological analysis of the *erg3* homozygote in vitro. The effect of *ERG3* disruption on the filamentous growth of *C. albicans* was monitored under known hyphae-inducing conditions (7, 21). CAF2-1 and the *Ura*⁺ *erg3* heterozygote, CAD1U, formed abundant hyphae under all tested conditions except YPD agar and RPMI 1640 broth (see Materials and Methods). In contrast, the *Ura*⁺ *erg3* homozygote, CAE3DU3, did not show a filamentous form including germ tube,

TABLE 3. Sterol compositions of *C. albicans* strains

Sterol	Sterol composition (%) without fluconazole treatment		
	CAI-4 (<i>ERG3/ERG3</i>)	CAD1 (<i>erg3/ERG3</i>)	CAE3D (<i>erg3/erg3</i>)
Ergosterol ^b	58.1	58.8	— ^a
Lanosterol ^c	10.4	9.6	2.0
Ergosta-7,22-dien-3β-ol	—	—	47.0
Episterol ^d or fecosterol ^e	—	—	9.8
4,4-Dimethyl-14-demethylated sterol ^f	8.4	6.8	10.3
Others	23.1	24.8	30.9

^a A bar (—) represents a sterol amount that was no more than 1%.

^b Ergosta-5,7,22-trien-3β-ol.

^c Lanosta-8,24-dien-3β-ol.

^d Ergosta-7,24(28)-dien-3β-ol.

^e Ergosta-8,24(28)-dien-3β-ol.

^f 4,4-Dimethyl-ergosta-8,14,24-trienol or 4,4-dimethyl-ergosta-8,24-dienol.

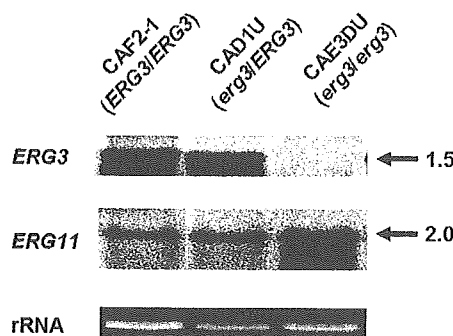


FIG. 2. Northern blot analysis of *ERG3* and *ERG11*. CAE3DU (*erg3/erg3*) showed a lack of *ERG3* transcript and increased *ERG11* expression compared to that of CAF2-1 (*ERG3/ERG3*) and CAD1U (*erg3/ERG3*). The visible rRNA bands serving as controls were approximately equivalent. The numbers to the right indicate the approximate sizes of mRNA in kilobases.

pseudohypha, and hypha under any of the tested conditions (data not shown).

Effects of the *ERG3* disruption on virulence in vivo. To clearly assess the effects of defective *ERG3* on virulence, survival and *C. albicans* burden in kidney tissue were monitored in mice intravenously inoculated with CAE3DU3, an *erg3/erg3* strain containing a copy of *URA3* at the native locus, versus CAF2-1 (*ERG3/ERG3 ura3/URA3*). Again, these paired strains showed the same growth rate at a variety of temperatures in vitro. Actual CFU (CFU/mouse) inoculated into mice for monitoring their survival were 0.904×10^6 and 4.52×10^5 for CAF2-1 and 0.922×10^6 and 4.61×10^5 for CAE3DU3. At both of higher and lower inoculum sizes, mice injected with CAE3DU3 survived significantly longer ($P < 0.001$ each) than those injected with CAF2-1 (Fig. 3).

To assess *C. albicans* burden in kidney tissue, both kidneys were excised on days 2, 4, and 7 of the experiment from mice infected with CAF2-1 or CAE3DU3 (Table 4). Inocula were 4.65×10^5 for CAF2-1 and 4.79×10^5 CFU/mouse for CAE3DU3. Concurrently, 10 mice of each inoculum group were monitored for survival. Survival curves of both groups

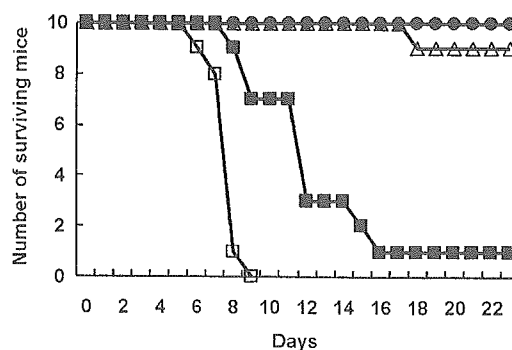


FIG. 3. Survival of mice infected with CAF2-1 (*ERG3/ERG3 ura3/URA3*) and CAE3DU3 (*erg3/erg3 ura3/URA3*). Immunocompetent mice ($n = 10$) were infected intravenously with 0.904×10^6 cells of CAF2-1 (open squares), 4.52×10^5 cells of CAF2-1 (solid squares), 0.922×10^6 cells of CAE3DU3 (open triangles), or 4.61×10^5 cells of CAE3DU3 (solid circles). Representative data of two independent experiments are shown.

TABLE 4. *C. albicans* burden in kidney tissue

Strain (genotype)	Inoculum (CFU/mouse)	Geometric mean \pm SD (\log_{10} CFU/g of kidney) ^a on day:		
		2	4	7
CAF2-1 (<i>ERG3/ERG3 ura3/URA3</i>)	4.65×10^5	4.40 ± 0.18	4.51 ± 0.15	5.09 ± 0.86
CAE3DU3 (<i>erg3/erg3 ura3/URA3</i>)	4.79×10^5	2.64 ± 1.55	2.82 ± 1.41	2.91 ± 1.31

^a Three mice per group on days 2 and 7 and four mice per group on day 4 were sacrificed for kidney removal. Results are expressed as the geometric mean \pm the standard deviation.

were consistent with the results shown in Fig. 3, and no mice died before day 8 of this experiment. Adjusted for the date of sacrifice, the mean log CFU of CAF2-1 was 1.86 (95% confidence interval, 0.91 and 2.81) higher (F test; $P = 0.001$) than that of CAE3DU3. The reduced virulence of CAE3DU3 was shown by both the longer survival (Fig. 3) and the lower kidney burdens (Table 4) of mice inoculated with this strain relative to CAF2-1.

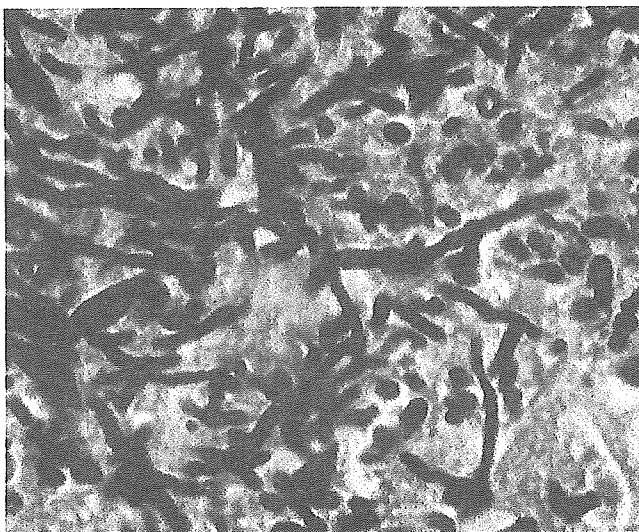
For histopathologic analysis, three mice per group were injected with CAF2-1 and CAE3DU3. Actual CFU (CFU/mouse) of each inoculum were 4.91×10^5 for CAF2-1 and 4.85×10^6 for CAE3DU3. Kidneys were excised 4 days after injection, and tissue sections were stained with Grocott-Gomori methenamine silver stain (Fig. 4). Kidney histopathology revealed that CAF2-1 cells formed abundant and intact hyphae, but almost all CAE3DU3 cells were blastospores. No intact hypha was detected, but aborted hyphal formation was observed in kidney tissues infected with CAE3DU3 (Fig. 4, arrows).

In vivo fluconazole susceptibility of the *ERG3* homozygote. Murine candidiasis caused by CAE3DU3 was treated with fluconazole to examine whether the *erg3* homozygote shows fluconazole resistance in vivo as observed in vitro. It is difficult

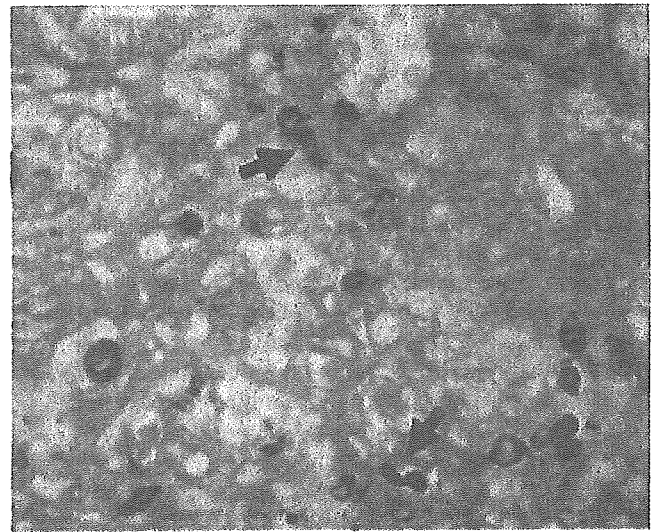
to assess drug efficacy between two strains having different virulence levels. Normally, it is easier to treat strains with low levels of virulence than those with high levels of virulence. In this study, therefore, mice were injected with CAE3DU3 (4.85×10^6 CFU/mouse) at a 10-fold higher concentration than CAF2-1 (4.91×10^5 CFU/mouse), and kidney CFU of both strains obtained from untreated groups were comparable ($P = 0.3$) (Fig. 5). No mice died until euthanasia for kidney removal on day 4. Fluconazole treatment by gavage at 40 mg/kg/day for 4 days after injection effectively reduced kidney CFU of CAF2-1 compared to that of the saline-treated group ($P < 0.0001$) (Fig. 5). Despite the fluconazole resistance measured by standard in vitro testing and a 10-fold higher inoculum compared to that of CAF2-1, kidney CFU of CAE3DU3 in the fluconazole-treated group was significantly less than that in the saline-treated group ($P < 0.0001$).

DISCUSSION

In this study, we interrupted both copies of *ERG3* in *C. albicans* and confirmed the known phenotypes, including in vitro azole resistance and the altered sterol profile. Novel find-



CAF2-1 (*ERG3/ERG3*)



CAE3DU3 (*erg3/erg3*)

FIG. 4. Histopathologic analysis of kidney tissues obtained from mice infected with CAF2-1 (*ERG3/ERG3 ura3/URA3*) and CAE3DU3 (*erg3/erg3 ura3/URA3*). Groups of three immunocompetent mice were infected intravenously with 4.91×10^5 cells of CAF2-1 or 4.85×10^6 cells of CAE3DU3. Kidneys were excised 4 days after injection, and tissue sections were stained with Grocott-Gomori methenamine silver stain. Note the aborted hyphal formation of CAE3DU3, shown in arrows, compared to abundant and intact hyphae of CAF2-1.

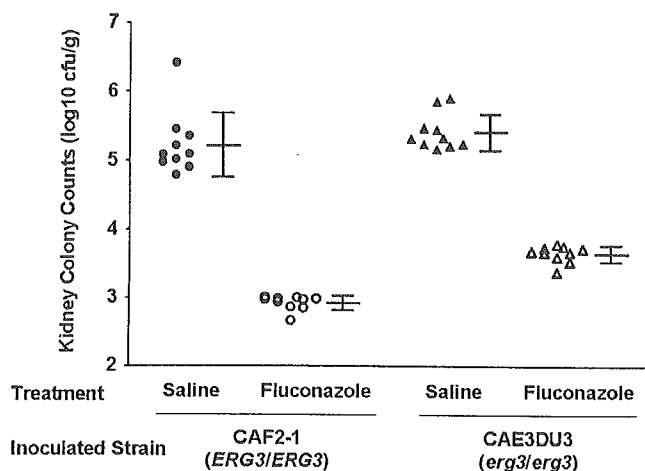


FIG. 5. Fluconazole treatment in a murine model of candidiasis. Immunocompetent mice ($n = 10$) were injected intravenously with 4.91×10^5 cells of CAF2-1 or 4.85×10^6 cells of CAE3DU3. Of note, the inoculum size of CAE3DU3 was 10-fold higher than that of CAF2-1 because of the difference in virulence between these strains. Fluconazole was administered by gavage at 40 mg/kg once a day for 4 days starting at 3 h after injection. Sterile saline was used as a control. Kidneys were excised 4 days after injection, and kidney CFU were determined. The scatter plot shows kidney CFU of CAF2-1 treated with saline (solid circles), CAF2-1 treated with fluconazole (open circles), CAE3DU3 treated with saline (solid triangles), and CAE3DU3 treated with fluconazole (open triangles). The geometric means and the standard deviations are shown in each group.

ings obtained from our *C. albicans erg3* homozygote were as follows: attenuated virulence in mice was accompanied by the reduction of kidney fungal burden and defective hyphal formation was observed in kidney tissues. Lastly, the *erg3* homozygote was susceptible to fluconazole in vivo.

The *erg3* homozygote showed no overexpression of *CDR1* and *MDR1* compared to the wild-type strain and contained no mutation in *ERG11*. The increased *ERG11* expression level observed in the *erg3* homozygote was consistent with previous reports (28, 33), except the report by Chau et al. (4). A feedback mechanism caused by the homozygous disruption of *ERG3*, which acts at the late phase (downstream of *ERG11*) in the ergosterol biosynthesis pathway, may account for the *ERG11* overexpression observed in the *erg3* homozygote. However, overexpression of *ERG11* is thought to have only a modest impact on azole resistance (31, 35).

To our knowledge, there is so far only one report addressing effects of defective C5,6-desaturase on morphology and virulence of *C. albicans* (4). In that report, no congenic strain was used as a control but defective filamentous growth of the *erg3* mutant in the presence of serum was shown, as confirmed here. The longer survival of mice infected with the mutant was not accompanied by a reduction of kidney fungal burdens, in contrast to our findings. Their failure to find a reduced fungal burden in the kidneys is probably due to the selection of a single and early time point 24 h after injection. In our study, a marked attenuation of virulence by *ERG3* disruption in *C. albicans* was equally evident from both the longer survival (Fig. 3) and the lower kidney burdens (Table 4) of mice inoculated with CAE3DU3 relative to the control strain, CAF2-1. In ad-

dition, we found a decreased ability of CAE3DU3 to form intact hyphae not only in vitro but in kidney tissues (Fig. 4). Our results obtained from in vivo experiments using female BALB/c mice and the control strain CAF2-1 were consistent with the data previously reported with that strain (22), indicating that an appropriate internal control had been selected.

Our experiment in mice also found that the fluconazole resistance of the *C. albicans erg3* homozygote could not be demonstrated in vivo (Fig. 4). To answer the question about the effect of fluconazole in the experimentally infected mouse, inoculum sizes of CAF2-1 and CAE3DU3 were chosen which provided a similar kidney burden. Under these conditions, kidney burdens of both strains were significantly decreased in the fluconazole-treated groups compared to the saline-treated control groups.

Of all our findings with the *erg3* homozygote, the most unexpected was the efficacy of fluconazole in a murine model of disseminated candidiasis. The inactivation of sterol C5,6-desaturase induced fluconazole resistance in vitro, consistent with the previous report (33). However, clinical significance of this resistance mechanism is still controversial, because only a few azole-resistant clinical isolates have exhibited a sterol profile indicative of defective sterol C5,6 desaturation (4, 18, 26). Information is limited because that mutation has not often been sought in clinical isolates. Another reason that such mutants may be rare in the infected host is the decreased virulence of such mutants. What is unclear is whether the *erg3* mutation alone contributes to clinically relevant resistance. Several studies in *C. albicans* have confirmed that multiple mechanisms are often involved in high-level resistance to fluconazole in an individual isolate. Both mutations in the *ERG11* gene and increased drug efflux are quite common (27, 35). Although a possibility remains that an *erg3* mutation spontaneously occurred in clinical settings and may have a role in azole resistance when combined with other mechanisms, this study suggests that an *erg3* mutation causing inactivation of sterol C5,6-desaturase is unlikely to confer in vivo fluconazole resistance by itself.

ACKNOWLEDGMENTS

We thank Yoko Kawamura for sterol assay, Chung-Yu Huang and Dean Follmann for statistical analyses, Katsunori Yanagihara, Yoichi Hirakata, and Kazunori Tomono for helpful discussion, and William A. Fonzi for pLUBP.

This research was supported by grants from the Japanese Ministry of Education (Grant-in-Aid for Scientific Research) and the Japanese Ministry of Health and Welfare and by the Intramural Research Program of the NIH, National Institute of Allergy and Infectious Diseases.

REFERENCES

- Anderson, J. B. 2005. Evolution of antifungal-drug resistance: mechanisms and pathogen fitness. *Nat. Rev. Microbiol.* 3:547-556.
- Aoyama, Y., Y. Yoshida, and R. Sato. 1984. Yeast cytochrome P-450 catalyzing lanosterol 14 alpha-demethylation. II. Lanosterol metabolism by purified P-450(14)DM and by intact microsomes. *J. Biol. Chem.* 259:1661-1666.
- Brand, A., D. M. MacCallum, A. J. Brown, N. A. Gow, and F. C. Odds. 2004. Ectopic expression of URA3 can influence the virulence phenotypes and proteome of *Candida albicans* but can be overcome by targeted reintegration of URA3 at the RPS10 locus. *Eukaryot. Cell* 3:900-909.
- Chau, A. S., M. Gurnani, R. Hawkinson, M. Laverdiere, A. Cacciapuoti, and P. M. McNicholas. 2005. Inactivation of sterol $\Delta^{5,6}$ -desaturase attenuates virulence in *Candida albicans*. *Antimicrob. Agents Chemother.* 49:3646-3651.
- Cheng, S., M. H. Nguyen, Z. Zhang, H. Jia, M. Handfield, and C. J. Clancy.

2003. Evaluation of the roles of four *Candida albicans* genes in virulence by using gene disruption strains that express URA3 from the native locus. *Infect. Immun.* 71:6101–6103.
6. **Committee on the Care and Use of Laboratory Animals of the Institute of Laboratory Animal Resources, Commission of Life Sciences, National Research Council.** 1996. Guide for the care and use of laboratory animals. National Academy Press, Washington, D.C.
 7. **Ernst, J. F.** 2000. Transcription factors in *Candida albicans* - environmental control of morphogenesis. *Microbiology* 146(Part 8):1763–1774.
 8. **Fonzi, W. A., and M. Y. Irwin.** 1993. Isogenic strain construction and gene mapping in *Candida albicans*. *Genetics* 134:717–728.
 9. **Geber, A., C. A. Hitchcock, J. E. Swartz, F. S. Pullen, K. E. Marsden, K. J. Kwon-Chung, and J. E. Bennett.** 1995. Deletion of the *Candida glabrata* ERG3 and ERG11 genes: effect on cell viability, cell growth, sterol composition, and antifungal susceptibility. *Antimicrob. Agents Chemother.* 39:2708–2717.
 10. **Gillum, A. M., E. Y. Tsay, and D. R. Kirsch.** 1984. Isolation of the *Candida albicans* gene for orotidine-5'-phosphate decarboxylase by complementation of *S. cerevisiae* *ura3* and *E. coli* *pyrF* mutations. *Mol. Gen. Genet.* 198:179–182.
 11. **Hemmi, K., C. Julmanop, D. Hirata, E. Tsuchiya, J. Y. Takemoto, and T. Miyakawa.** 1995. The physiological roles of membrane ergosterol as revealed by the phenotypes of *syrl/erg3* null mutant of *Saccharomyces cerevisiae*. *Biosci. Biotechnol. Biochem.* 59:482–486.
 12. **Henry, K. W., J. T. Nickels, and T. D. Edlind.** 2000. Upregulation of ERG genes in *Candida* species by azoles and other sterol biosynthesis inhibitors. *Antimicrob. Agents Chemother.* 44:2693–2700.
 13. **Hitchcock, C. A., K. Dickinson, S. B. Brown, E. G. Evans, and D. J. Adams.** 1989. Purification and properties of cytochrome P-450-dependent 14 alpha-sterol demethylase from *Candida albicans*. *Biochem. J.* 263:573–579.
 14. **Johnson, E. M., D. W. Warnock, J. Luker, S. R. Porter, and C. Scully.** 1995. Emergence of azole drug resistance in *Candida* species from HIV-infected patients receiving prolonged fluconazole therapy for oral candidosis. *J. Antimicrob. Chemother.* 35:103–114.
 15. **Kakeya, H., Y. Miyazaki, H. Miyazaki, K. Nyswaner, B. Grimberg, and J. E. Bennett.** 2000. Genetic analysis of azole resistance in the Darlington strain of *Candida albicans*. *Antimicrob. Agents Chemother.* 44:2985–2990.
 16. **Kelly, R., S. M. Miller, M. B. Kurtz, and D. R. Kirsch.** 1987. Directed mutagenesis in *Candida albicans*: one-step gene disruption to isolate *ura3* mutants. *Mol. Cell. Biol.* 7:199–208.
 17. **Kelly, S. L., D. C. Lamb, A. J. Corran, B. C. Baldwin, and D. E. Kelly.** 1995. Mode of action and resistance to azole antifungals associated with the formation of 14 alpha-methylergosta-8,24(28)-dien-3 beta,6 alpha-diol. *Biochem. Biophys. Res. Commun.* 207:910–915.
 18. **Kelly, S. L., D. C. Lamb, D. E. Kelly, N. J. Manning, J. Loeffler, H. Hebart, U. Schumacher, and H. Einsele.** 1997. Resistance to fluconazole and cross-resistance to amphotericin B in *Candida albicans* from AIDS patients caused by defective sterol delta5,6-desaturation. *FEBS Lett.* 400:80–82.
 19. **Lay, J., L. K. Henry, J. Clifford, Y. Koltin, C. E. Bulawa, and J. M. Becker.** 1998. Altered expression of selectable marker URA3 in gene-disrupted *Candida albicans* strains complicates interpretation of virulence studies. *Infect. Immun.* 66:5301–5306.
 20. **Limjindaporn, T., R. A. Khalaf, and W. A. Fonzi.** 2003. Nitrogen metabolism and virulence of *Candida albicans* require the GATA-type transcriptional activator encoded by GAT1. *Mol. Microbiol.* 50:993–1004.
 21. **Liu, H., J. Kohler, and G. R. Fink.** 1994. Suppression of hyphal formation in *Candida albicans* by mutation of a STE12 homolog. *Science* 266:1723–1726.
 22. **MacCallum, D. M., and F. C. Odds.** 2005. Temporal events in the intravenous challenge model for experimental *Candida albicans* infections in female mice. *Mycoses* 48:151–161.
 23. **Marr, K. A., T. R. Rustad, J. H. Rex, and T. C. White.** 1999. The trailing end point phenotype in antifungal susceptibility testing is pH dependent. *Antimicrob. Agents Chemother.* 43:1383–1386.
 24. **Miyazaki, Y., A. Geber, H. Miyazaki, D. Falconer, T. Parkinson, C. Hitchcock, B. Grimberg, K. Nyswaner, and J. E. Bennett.** 1999. Cloning, sequencing, expression and allelic sequence diversity of ERG3 (*C-5* sterol desaturase gene) in *Candida albicans*. *Gene* 236:43–51.
 25. **National Committee for Clinical Laboratory Standards.** 2002. Reference method for broth dilution antifungal susceptibility testing of yeasts; approved standard, 2nd ed. NCCLS document M27-A2. National Committee for Clinical Laboratory Standards, Wayne, Pa.
 26. **Nolte, F. S., T. Parkinson, D. J. Falconer, S. Dix, J. Williams, C. Gilmore, R. Geller, and J. R. Wingard.** 1997. Isolation and characterization of fluconazole- and amphotericin B-resistant *Candida albicans* from blood of two patients with leukemia. *Antimicrob. Agents Chemother.* 41:196–199.
 27. **Perea, S., J. L. Lopez-Ribot, W. R. Kirkpatrick, R. K. McAtee, R. A. Santillan, M. Martinez, D. Calabrese, D. Sanglard, and T. F. Patterson.** 2001. Prevalence of molecular mechanisms of resistance to azole antifungal agents in *Candida albicans* strains displaying high-level fluconazole resistance isolated from human immunodeficiency virus-infected patients. *Antimicrob. Agents Chemother.* 45:2676–2684.
 28. **Pierson, C. A., J. Eckstein, R. Barbuch, and M. Bard.** 2004. Ergosterol gene expression in wild-type and ergosterol-deficient mutants of *Candida albicans*. *Med. Mycol.* 42:385–389.
 29. **Rex, J. H., P. W. Nelson, V. L. Paetznick, M. Lozano-Chiu, A. Espinel-Ingroff, and E. J. Anaissie.** 1998. Optimizing the correlation between results of testing in vitro and therapeutic outcome in vivo for fluconazole by testing critical isolates in a murine model of invasive candidiasis. *Antimicrob. Agents Chemother.* 42:129–134.
 30. **Sambrook, J., and W. Russell (ed.).** 2001. Molecular cloning: a laboratory manual, 3rd ed. Cold Spring Harbor Laboratory Press, Cold Spring Harbor, N.Y.
 31. **Sanglard, D.** 2002. Resistance of human fungal pathogens to antifungal drugs. *Curr. Opin. Microbiol.* 5:379–385.
 32. **Sanglard, D., F. Ischer, M. Monod, and J. Bille.** 1997. Cloning of *Candida albicans* genes conferring resistance to azole antifungal agents: characterization of CDR2, a new multidrug ABC transporter gene. *Microbiology* 143(Part 2):405–416.
 33. **Sanglard, D., F. Ischer, T. Parkinson, D. Falconer, and J. Bille.** 2003. *Candida albicans* mutations in the ergosterol biosynthetic pathway and resistance to several antifungal agents. *Antimicrob. Agents Chemother.* 47:2404–2412.
 34. **Sanglard, D., K. Kuchler, F. Ischer, J. L. Pagani, M. Monod, and J. Bille.** 1995. Mechanisms of resistance to azole antifungal agents in *Candida albicans* isolates from AIDS patients involve specific multidrug transporters. *Antimicrob. Agents Chemother.* 39:2378–2386.
 35. **Sanglard, D., and F. C. Odds.** 2002. Resistance of *Candida* species to antifungal agents: molecular mechanisms and clinical consequences. *Lancet Infect. Dis.* 2:73–85.
 36. **Staab, J. F., and P. Sundstrom.** 2003. URA3 as a selectable marker for disruption and virulence assessment of *Candida albicans* genes. *Trends Microbiol.* 11:69–73.
 37. **Vanden Bossche, H., P. Marichal, J. Gorrens, D. Bellens, H. Moereels, and P. A. Janssen.** 1990. Mutation in cytochrome P-450-dependent 14 alpha-demethylase results in decreased affinity for azole antifungals. *Biochem. Soc. Trans.* 18:56–59.
 38. **Vanden Bossche, H., P. Marichal, and F. C. Odds.** 1994. Molecular mechanisms of drug resistance in fungi. *Trends Microbiol.* 2:393–400.
 39. **Varma, A., J. C. Edman, and K. J. Kwon-Chung.** 1992. Molecular and genetic analysis of URA5 transformants of *Cryptococcus neoformans*. *Infect. Immun.* 60:1101–1108.
 40. **Vuffray, A., C. Durussel, P. Boerlin, F. Boerlin-Petzold, J. Bille, M. P. Glauser, and J. P. Chave.** 1994. Oropharyngeal candidiasis resistant to single-dose therapy with fluconazole in HIV-infected patients. *AIDS* 8:708–709.
 41. **White, T. C., S. Holleman, F. Dy, L. F. Mirels, and D. A. Stevens.** 2002. Resistance mechanisms in clinical isolates of *Candida albicans*. *Antimicrob. Agents Chemother.* 46:1704–1713.

3年間研究成果（北村 唯一）の
に関する一覧表

雑誌

発表者氏名		論文タイトル名			
Zheng H.-Y., Kitamura T., Takasaka T., Chen Q., and Yogo Y.	Unambiguous identification of JC polyomavirus strains transmitted from parents to children.	Arch. Virol.	149	261-273	2004
Zheng H.-Y., Yasuda Y., Kato S., Kitamura T., and Yogo Y.	Stability of JC virus-coding sequences in a case of progressive multifocal leukoencephalopathy where the viral control region was rearranged markedly.	Arch. Pathol. Lab. Med.	128	275-278	2004
Zheng H.-Y., Zhao P., Suganami H., Ohasi Y., Ikegaya H., Kim J.C., Sugimoto C., Takasaka T., Kitamura T., and Yogo Y.:	Regional distribution of two related Northeast Asian genotypes of JC virus, CY-a and -b: implications for the dispersal of Northeast Asians.	Microbes Infect.	6	596-603	2004
Yogo Y., Sugimoto C., Zheng H.-Y., Ikegaya H., Takasaka T., and Kitamura T.	JC virus genotyping offers a new paradigm in the study of human populations.	Rev. Med. Virol.	14	179-191	2004
Kato A., Kitamura T., Takasaka T., Zheng H.-Y., Tominaga T., and Yogo Y.	Detection of the archetypal regulatory region of JC virus from the tonsil tissue of patients with tonsillitis and tonsillar hypertrophy.	J. Neurovirol.	10	244-249	2004
Takasaka T., Goya N., Tokumoto T., Tanabe K., Toma H., Ogawa Y., Hokama S., Momose A., Funyu T., Fujioka T., Omori S., Akiyama H., Chen Q., Zheng H.-Y., Ohta N., Kitamura T., and Yogo Y.	Subtypes of BK virus prevalent in Japan and variation in their transcriptional control region.	J. Gen. Virol.	85	2821-2827	2004
Takasaka A., Miranda J.J., Sugimoto C., Paraguison R., Zheng H.-Y., Kitamura T., and Yogo Y.	Genotypes of JC Virus in Southeast Asia and the Western Pacific: Implications for Human Migrations from Asia to the Pacific.	Anthropol. Sci.	112	53-59	2004
Miranda J.J., Takasaka T., Zheng H.-Y., Kitamura T., and Yogo Y.	JC virus genotype profile in the Mamanwa, a Philippine Negrito tribe, and implications for its population history.	Anthropol. Sci.	112	173-178	2004
Zheng H.-Y., Takasaka T., Noda K., Kanazawa A., Mori H., Kabuki T., Joh K., Oh-ishi T., Ikegaya H., Nagashima K., Hall W.W., Kitamura T., and Yogo Y.	New sequence polymorphisms in the outer loops of the JC polyomavirus major capsid protein (VP1) possibly associated with progressive multifocal leukoencephalopathy.	J. Gen. Virol.	86	2035-2045	2005
Zheng H.-Y., Ikegaya H., Takasaka T., Matsushima-Ohno T., Sakurai M., Kanazawa I., Kishida S., Nagashima K., Kitamura T., and Yogo Y.	Characterization of the VP1 loop mutations widespread among JC polyomavirus isolates associated with progressive multifocal leukoencephalopathy.	Biochem. Biophys. Res. Commun.	333	996-1002	2005
Zheng H.-Y., Ikegaya H., Nakajima M., Sakurada K., Takasaka T., Kitamura T., and Yogo Y.	Two distinct genotypes (MY-x and MX) of JC virus previously identified in Hokkaido Ainu.	Anthropol. Sci.	113	225-231	2005
Zheng H.-Y., Kojima K., Ikegaya H., Takasaka T., Kitamura T., and Yogo Y.	JC virus genotyping suggests a close contact or affinity between Greenland Inuit and other circumpolar populations.	Anthropol. Sci.	113	291-293	2005
Ikegaya H., Zheng H.-Y., Saukko P.J., Varesmaa-Korhonen L., Hovi T., Vesikari T., Suganami H., Takasaka T., Sugimoto C., Ohasi Y., Kitamura T., and Yogo Y.	Genetic diversity of JC virus in the Saami and the Finns: Implications for their population history.	Am. J. Phys. Anthropol.	128	185-193	2005
Ikegaya H., Iwase H., Zheng H.-Y., Nakajima M., Sakurada K., Takatori T., Fukayama M., Kitamura T., and Yogo Y.	JC virus genotyping using formalin-fixed, paraffin-embedded renal tissues.	J. Virol. Methods	126	37-43	2005
Takasaka T., Goya N., Ishida H., Tanabe K., Toma H., Fujioka T., Omori S., Zheng H.-Y., Chen Q., Nukuzuma S., Kitamura T., and Yogo Y.	Stability of the BK polyomavirus genome in renal transplant patients without nephropathy.	J. Gen. Virol.	87	303-306	2006
Takasaka T., Kitamura T., Sugimoto C., Guo J., Zheng H.-Y., and Yogo Y.	Phylogenetic analysis of the major African genotype (A β) of JC virus: Implications for the origin and dispersals of modern Africans.	Am. J. Phys. Anthropol.	129	465-472	2006
Takasaka T., Ohta N., Zheng H.-Y., Ikegaya H., Sakurada K., Kitamura T., and Yogo Y.	JC polyomavirus lineages common among Kiribati Islanders: implications for human dispersal in the Pacific.	Anthropol. Sci.			2006 in press.
Saruwatari L., Zheng H.-Y., Takasaka T., Guo J., Kitamura T., Yogo Y., and Ohno N.	Dispersal of southeastern Asians based on the phylogenetic analysis of JC virus isolates worldwide belonging to genotype SC.	Anthropol. Sci.			2006 in press.

Unambiguous identification of *JC polyomavirus* strains transmitted from parents to children

H.-Y. Zheng, T. Kitamura, T. Takasaka, Q. Chen, and Y. Yogo

Department of Urology, Faculty of Medicine, The University of Tokyo,
Tokyo, Japan

Received May 9, 2003; accepted August 20, 2003

Published online October 30, 2003 © Springer-Verlag 2003

Summary. *JC polyomavirus* (JCV), the etiological agent of progressive multifocal leukoencephalopathy, is ubiquitous in humans, infecting children asymptotically, then persisting in renal tissue. It has been proposed that JCV is transmitted mainly from parents to children through long-term cohabitation. The objective of this study was to further elucidate the mode of JCV transmission. In 5 families, we selected parent/child pairs between whom JCV was probably transmitted (judged on the basis of the identity of a 610-bp JCV DNA sequence between the parent and child). We established 5 to 9 complete JCV DNA clones from the urine of each parent or child. The complete sequences of these clones were determined and compared in each family. Nucleotide substitutions were detected in 4 parents and 1 child, and sequence rearrangements (deletions or duplications) were found in 2 parents and 2 children. Phylogenetic comparison of the detected sequences indicated that the diversity of JCV DNA sequences was generated in each family (i.e. not caused by multiple infection). We found that in 4 of the 5 families, a sequence detected in the parent was completely identical to one in the child. These findings provided further support for the proposed mode of JCV transmission, i.e. parent-to-child transmission during cohabitation.

Introduction

JC polyomavirus (JCV) is the causative agent of a fatal demyelinating disease in the central nervous system, known as progressive multifocal leukoencephalopathy (PML) [26, 29]. However, this virus is ubiquitous in the human population. Primary infection usually occurs asymptotically during childhood [30, 40]. JCV persists in the kidney of most adults, who excrete progeny viruses in urine [1, 9, 20, 22, 39]. JCV may also persist in other sites, including peripheral blood lymphocytes, lymphoid tissues, and the central nervous system [11].

Serological studies [10, 30, 37, 40] have shown that children are infected with JCV after birth (i.e. JCV transmission is categorized as horizontal [28]). Using urinary JCV DNA, several attempts have been made to further elucidate the mode of JCV transmission. (i) Kunitake et al. [24] PCR-amplified a 610-bp JCV DNA region (IG region) from urine specimens collected from all members of 7 families. (The IG region was previously established as a region of the JCV DNA that contains relatively abundant sites for typing JCV DNAs [7].) JCV strains were identified by the nucleotide sequences of the amplified IG regions. Strains detected in half of the JCV-positive children were identified in their parents. Furthermore, Kunitake et al. [24] detected the same IG sequences in the offspring as well as in the fathers (3 cases) or mothers (3 cases) of the 6 families, suggesting that JCV transmission occurs both maternally and paternally. (ii) Kato et al. [17] studied whether JCV have been transmitted from the American population to the Japanese population both existing on a small island, Okinawa, Japan. No American JCV genotypes were detected in the Japanese population. (iii) Suzuki et al. [36] collected urine samples in Los Angeles from second and third generation Japanese-Americans whose parents and grandparents were all Japanese. From these urine samples, 2 genotypes (CY and MY) of JCV that predominantly occur in homeland Japanese [23] were mainly detected in each generation of the Japanese-Americans. Taken these findings together, it is likely that JCV is transmitted mainly from parents to children during long-term cohabitation.

In this study, we attempted to gain further insights into the transmission of JCV. We selected 5 families in each of which JCV was probably transmitted from a parent to a child (2 children in a single family). This judgment was made on the basis of the identity of the 610-bp IG sequence between the parent and child. At least 5 complete JCV DNA clones were established and sequenced from the urine of each parent or child. Although JCV DNA sequences significantly varied in most families, we detected a completely identical JCV DNA sequence in both the parent and the child belonging to each of 4 families. These findings provided support for the proposed mode of JCV transmission, i.e. parent-to-child transmission during cohabitation.

Materials and methods

Subjects

Five families were studied (Table 1). Families A to C were previously studied by Kunitake et al. [24] (families A, B, and C corresponded to families 3, 2, and 5, respectively, studied by Kunitake et al. [24]). Families D and E were first investigated in this study. A parent/child pair (2 children in family A) was selected in each family on the basis of the identity of the 610-bp IG sequence detected in their urine. All subjects were immunocompetent.

DNA analysis

Entire JCV DNAs were cloned into pUC19 at the unique *Bam*HI site as described previously [42]. The resultant complete JCV DNA clones were prepared using a QIAGEN Plasmid Midi

Table 1. Parents and children included in this study^a

Family	Member	Age (yr)	No. of clones analyzed
A	Parent (father) ^b	52	6
A	Child 1 (daughter)	29	5
A	Child 2 (daughter)	26	5
B	Parent (mother) ^c	84	6
B	Child (daughter)	59	6
C	Parent (father) ^b	86	9
C	Child (son)	60	5
D	Parent (mother) ^d	56	5
D	Child (son)	26	5
E	Parent (mother) ^d	62	5
E	Child (son)	25	5

^aA parent/child pair (2 children in family A) was selected in each family on the basis of the identity of the 610-bp IG sequence detected in their urine

^bJCV DNA was not detected in the mother

^cNo information on the JCV DNA sequence in the father was available because of his death

^dThe 610-bp IG sequence in the father significantly diverged from that in the child

kit (QIAGEN GmbH, Hilden, Germany). Purified plasmids were sequenced as described previously [35].

Phylogenetic analysis

The noncoding regulatory region of the JCV genome was excluded from phylogenetic analysis, as this region is hypervariable especially in JCV isolates derived from the brains of PML patients [16, 41, 43]. The determined and reference sequences were aligned using the CLUSTAL W program [38]. The aligned sequences were subjected to phylogenetic analysis using the neighbor-joining (NJ) method [32]. Phylogenetic trees were constructed using CLUSTAL W, and divergences were estimated by the 2-parameter method [19]. Phylogenetic trees were visualized using TREEVIEW [31]. To assess the confidence of branching patterns of the NJ trees, 1,000 bootstrap replications were performed [12]. Bootstrap probabilities larger than 70% were considered to be significant [15].

Results

Sequences detected in each family

We attempted to establish complete JCV DNA clones from urine samples collected from parents and children belonging to families A to E. We obtained 5 to 9 complete JCV DNA clones from each subject (Table 1). We sequenced all of these clones and deposited the obtained sequences in GSDB, EMBL, DDBJ, and NCBI nucleotide sequence databases with the accession numbers indicated in Table 2.

Two sequences, FA-1 and FA-1a, were detected in family A (Table 3). In reference to FA-1, FA-1a carried a 63-bp deletion within the VP2/3 gene spanning

Table 2. Complete JCV DNA sequences determined in this study

Family	Sequence	Genotype	Accession no. ^a
A	FA-1	B1-b	AB103387
A	FA-1a	B1-b	AB103402
B	FB-1	MY-b	AB103403
B	FB-2	MY-b	AB103404
B	FB-3	MY-b	AB103405
C	FC-1	CY	AB103406
C	FC-1a	CY	AB103407
C	FC-2	CY	AB103408
C	FC-3	CY	AB103409
C	FC-3a	CY	AB104487
C	FC-4	CY	AB103410
C	FC-4a	CY	AB103411
C	FC-5	CY	AB103412
D	FD-1	MY-b	AB103413
D	FD-1a	MY-b	AB103414
D	FD-2	MY-b	AB103415
D	FD-3	MY-b	AB103416
E	FE-1	CY	AB103417
E	FE-2	CY	AB103418
E	FE-3	CY	AB103419
– ^b	HA ^c	MY-b	AB103420
–	HS ^c	MY-b	AB103421
–	KF ^c	MY-b	AB103422
–	ST ^c	MY-b	AB103423

^aGSDB, EMBL, DDBJ, and NCBI nucleotide sequence databases

^bUnrelated to families A–E

^cClones previously established [40]

Table 3. Comparison and distribution of complete JCV DNA sequences detected in family A

Sequence	Rearrangement	No. of clones with the indicated sequence in:		
		Parent	Child 1	Child 2
FA-1	– ^a	6	5	4
FA-1a	del ^b	0	0	1

^aNone

^bDeletion of a 63-bp sequence (nt 1281–1343) within the VP2/3 gene

from nucleotide (nt) 1281 to 1343 (nucleotide numbers are those of an archetype isolate, CY [18], starting from the midpoint of the origin of replication and proceeding clockwise). All clones from the parent and child 1 and most clones from child 2 contained FA-1, while a single clone from child 2 had FA-1a.

Table 4. Comparison and distribution of complete JCV DNA sequences detected in family B

Sequence	Nucleotide substitution at:		Rearrangement	No. of clones with the indicated sequence in:	
	nt 1667	nt 4109		Parent	Child
FB-1	A	A	— ^a	3	0
FB-2	G	A	—	2	6
FB-3	G	G	—	1	0

^aNone**Table 5.** Comparison and distribution of complete JCV DNA sequences detected in family C

Sequence	Nucleotide substitution at:				Rearrangement	No. of clones with the indicated sequence in:	
	nt 2612	nt 3065	nt 3202	nt 3310		Parent	Child
FC-1	G	G	A	A	— ^a	0	4
FC-1a	G	G	A	A	del ^b	0	1
FC-2	G	G	A	T	—	1	0
FC-3	G	A	A	A	—	2	0
FC-3a	G	A	A	A	dup ^c	1	0
FC-4	G	G	C	A	—	3	0
FC-4a	G	G	C	A	dup ^d	1	0
FC-5	T	G	A	G	—	1	0

^aNone^bDeletion of a 38-bp segment (nt 4931–4968) within the LT exon^cDuplication of a 36-bp segment (nt 204–239) within the regulatory region^dDuplication of a 52-bp segment (nt 212–263) within the regulatory region

Three sequences, FB-1 to -3, were detected in family B (Table 4). These sequences were distinguishable by nucleotide substitutions at 2 sites, nt 1667 and 4109, within the VP1 and large T antigen (abbreviated as LT) genes, respectively. FB-1 to -3 were found in the parent, but only FB-2 was found in the child.

Eight sequences, FC-1, -1a, -2, -3, -3a, -4, -4a, and -5, were detected in family C (Table 5). These sequences were distinguishable by substitutions at 4 sites, nt 2612, 3065, 3202, and 3310, all locating within the LT gene, and by a 38-bp deletion within the LT gene, and 36-bp and 52-bp duplications within the regulatory region. Six sequences (FC-2, -3, -3a, -4, -4a, and -5) were found in the parent, and 2 sequences (FC-1 and FC-1a) were found in the child.

Four sequences, FD-1, -1a, -2, and -3, were detected in family D (Table 6). These sequences were distinguishable by nucleotide substitutions at 2 sites, nt 2933 and 3308, within the LT gene and by a 28-bp deletion within the regulatory

Table 6. Comparison and distribution of complete JCV DNA sequences detected in family D

Sequence	Nucleotide substitution at:		Rearrangement	No. of clones with the indicated sequence in:	
	nt 2933	nt 3308		Parent	Child
FD-1	C	A	– ^a	2	5
FD-1a	C	A	del ^b	1	0
FD-2	C	T	–	1	0
FD-3	T	A	–	1	0

^aNone^bDeletion of a 28-bp segment (nt 217–244) within the regulatory region. This deletion accompanied 3 nucleotide substitutions at nt 245, 247, and 253**Table 7.** Comparison and distribution of complete JCV DNA sequences detected in family E

Sequence	Nucleotide substitution at:		Rearrangement	No. of clones with the indicated sequence in:	
	nt 3225	nt 3308		Parent	Child
FE-1	G	A	– ^a	2	4
FE-2	G	C	–	3	0
FE-3	A	A	–	0	1

^aNone

region. All of the four sequences were found in the parent, but only FD-1 was found in the child.

Three sequences, FE-1 to -3, were detected in family E (Table 7). These sequences were distinguishable by substitutions at 2 sites, nt 3225 and 3308, within the VP1 and LT genes, respectively. FE-1 and -2 were found in the parent, and FE-1 and -3 were found in the child.

Genotyping JCV DNA sequences detected in the 5 families

The JCV strains in the world constitute a single serotype [26]. However, they are classified into more than ten subtypes (also designated genotypes) based on nucleotide differences among them [6]. To classify detected JCV DNA sequences into genotypes, we constructed a NJ phylogenetic tree from 17 complete JCV DNA sequences detected in the 5 families together with 64 complete JCV DNA sequences reported previously [2–5, 13, 18, 25, 35]. According to the resultant tree (not shown), (i) the JCV DNA sequences detected in family A belonged to genotype B1-b; (ii) those detected in families B and D belonged to genotype

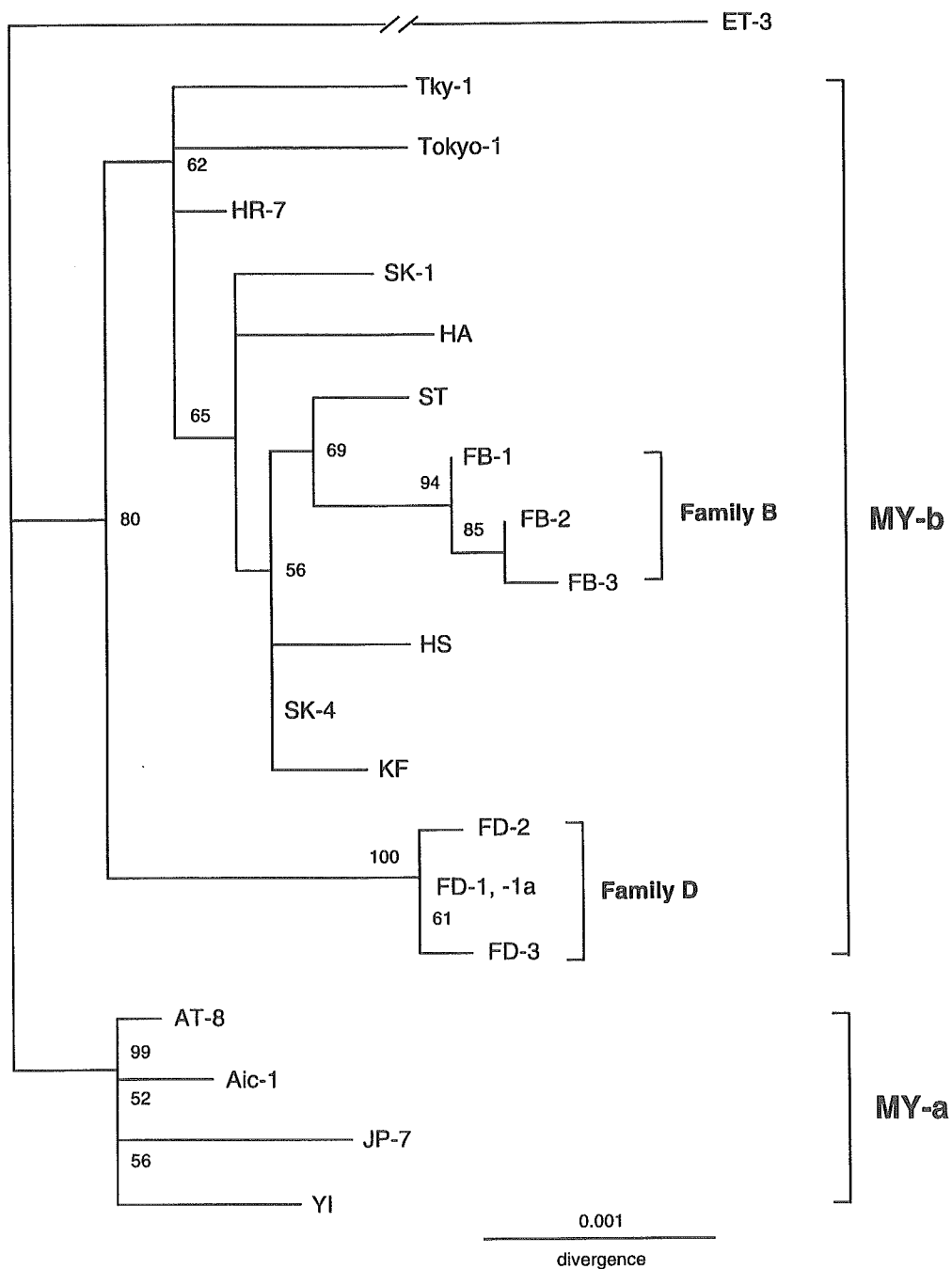


Fig. 1. NJ phylogenetic tree relating complete JCV DNA sequences detected in families B and D. A NJ phylogenetic tree was constructed from 6 complete MY-a/-b sequences detected in families B and D and 13 complete MY sequences detected in unrelated individuals (11 Japanese and 2 Koreans) [4, 18, 35, 44, and Table 2] (the noncoding regulatory region of the JCV genome was excluded from this phylogenetic analysis). The phylogenetic tree was visualized using TREEVIEW. The tree was rooted using a genotype Af2 isolate (ET-3) [35] as the outgroup. The symbols for isolates are shown in Table 2 and described elsewhere [4, 18, 35, 44]. The numbers at nodes in the tree indicate the bootstrap confidence levels (percent) obtained with 1,000 replications (only values $\geq 50\%$ are shown)

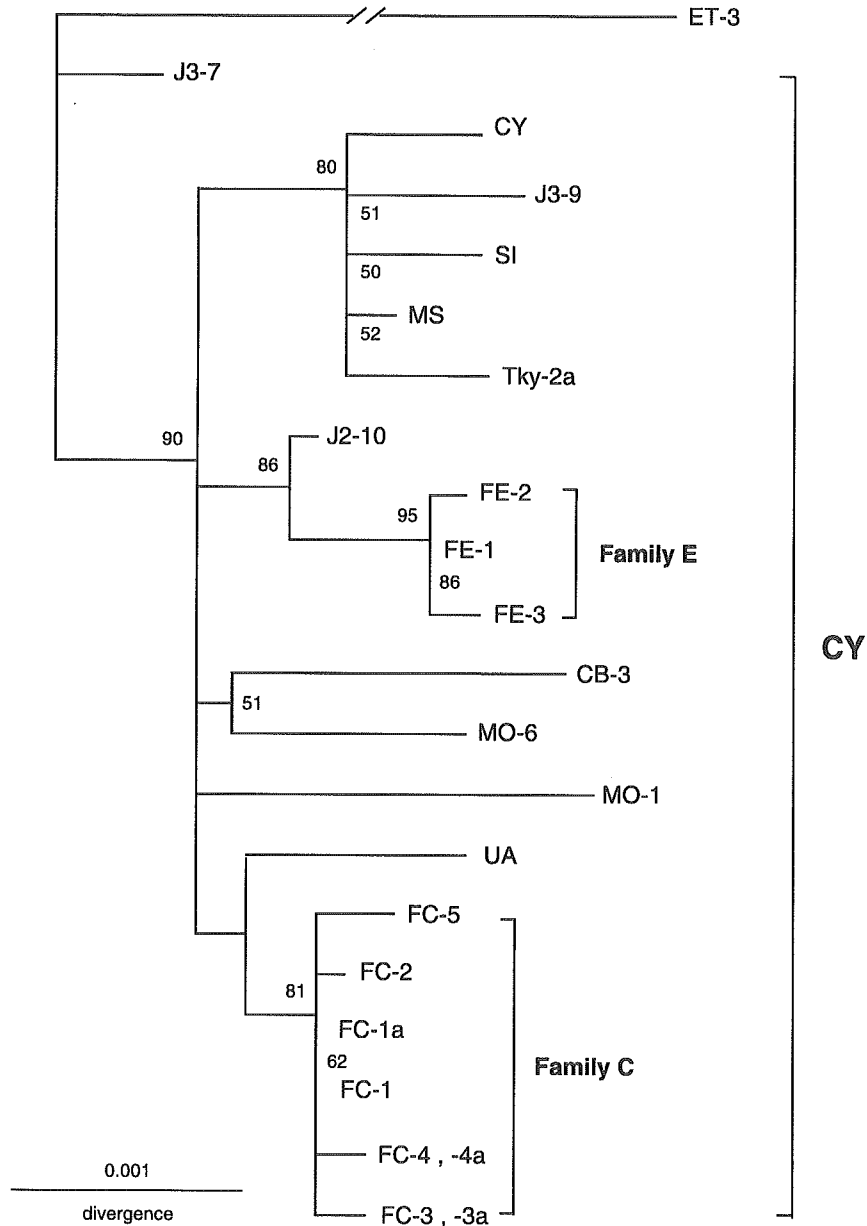


Fig. 2. NJ phylogenetic tree relating complete JCV DNA sequences detected in families C and E. A NJ phylogenetic tree was constructed from 11 complete CY sequences detected in families C and E and 11 complete CY sequences detected in unrelated individuals (6 Japanese, 3 Japanese Americans, 2 Mongolians, and 1 Chinese [18, 35, 36]). The phylogenetic tree was visualized using TREEVIEW. The tree was rooted using a genotype Af2 isolate (ET-3) [35] as the outgroup. The symbols for isolates are shown in Table 2 and described elsewhere [18, 35, 36]. The numbers at nodes in the tree indicate the bootstrap confidence levels (percent) obtained with 1,000 replications (only values $\geq 50\%$ are shown)

MY-b; and (iii) those detected in families C and E belonged to genotype CY. B1-b is mainly prevalent in Central and Western Asia [34], but is rarely detected in Japan [23]. MY-b and CY are both prevalent in Japan [23].

Phylogenetic comparison of JCV DNA sequences in each family

As described above, all JCV DNA sequences detected in families B and D belonged to genotype MY. These sequences together with 13 complete MY-a/-b DNA sequences identified in unrelated subjects, including 11 in Japanese and 2 in South Koreans [18, 35, 44, and Table 2], were used to construct a NJ phylogenetic tree (Fig. 1). All JCV DNA sequences detected in families C and E belonged to genotype CY. These sequences together with 11 complete MY DNA sequences previously reported, including 5 in Japanese, 3 in Japanese-Americans, 2 in Mongolians, and 1 in a Chinese [18, 35, 36], were used to construct a NJ phylogenetic tree (Fig. 2). On the resultant trees (Figs. 1 and 2), all sequences detected in each family clustered together at a bootstrap probability of 75–100%. As bootstrap probabilities larger than 70% can be considered to be significant [15], the above result suggests that all JCV DNA sequences in each family were phylogenetically related.

Alteration in the amino acid sequences of viral proteins

Nucleotide substitutions detected in JCV DNA sequences and amino acid substitutions predicted by them are shown in reference to prototypical sequences

Table 8. Amino acid substitutions caused by nucleotide substitutions in complete JCV DNA clones

JCV DNA sequences	Site of the JCV genome (gene)	Nucleotide substitution ^a	Amino acid substitution ^b
FB-2, -3	nt 1667 (VP1)	A/G	— ^c
FB-3	nt 4109 (LT)	A/G	—
FC-2	nt 3310 (LT)	A/T	—
FC-3, -3a	nt 3065 (LT)	G/A	S/L
FC-4, -4a	nt 3202 (LT)	A/C	—
FC-5	nt 2612 (LT)	G/T	T/N
FC-5	nt 3310 (LT)	A/G	—
FD-2	nt 3308 (LT)	A/T	—
FD-3	nt 2933 (LT)	C/T	—
FE-2	nt 3308 (LT)	A/C	—
FE-3	nt 3225 (LT)	G/A	T/I

^a[nucleotide in the indicated JCV DNA sequence]/[nucleotide in the hypothetical prototypical JCV DNA sequence] (see text)

^b[amino acid in the LT encoded by the indicated JCV DNA sequence]/[amino acid in the LT encoded by the hypothetical prototypical JCV DNA sequence] (see text)

^cNone